Chapter

Local Scour around a Monopile Foundation for Offshore Wind Turbines and Scour Effects on Structural Responses

Wen-Gang Qi and Fu-Ping Gao

Abstract

Monopile is the most commonly used foundation type for offshore wind turbines. The local scour at a monopile foundation generated by the incoming shear flow has significant influence on both quasi-static lateral responses and dynamic responses of the monopile. This chapter focuses particularly on characterizing the local scour in both spatial and temporal scales and revealing the scour mechanisms associated with the flow field around a monopile. The predicting methods for the equilibrium scour depth and the time scale of scour are detailed under various representative flow conditions in the marine environment. The scale effect while extrapolating the results of model tests to prototype conditions is highlighted. The local scour imposes significant influence not only on the deformation and stiffness of the monopile foundation, but also on the natural frequency and fatigue life of the structure system. Monopiles with diameters up to 10 m have become a feasible option as the industry is currently advancing into deeper waters. More meticulous considerations for monopile design associated with the scour depth prediction and evaluation of scour effects are still in need to efficiently minimize the cost while remaining safety simultaneously.

Keywords: local scour, monopile, combined waves and currents, horseshoe vortex, time scale, backfilling, scale effect, pile-soil interaction, natural frequency

1. Introduction

Offshore wind power is developing into a major energy source globally due to the abundant reserves, high-energy density, and fewer civil complaints compared to onshore wind power. The global installed capacity reached more than 14,300 MW at the end of 2016 [1], and an increased potential for growth in future was estimated [2, 3]. To achieve high energy harvesting efficiency, the industry is currently advancing into deeper waters accompanied by upscaling the offshore wind turbines (OWTs) from 5 to 8 MW, 10 MW and then 12 MW [4] (see **Figure 1**). The steady upward trends in both water depth and size of OWTs have led to consequential growth in the loading, further aggravating the deformation of the foundations and potentially jeopardizing the operation of the OWTs.

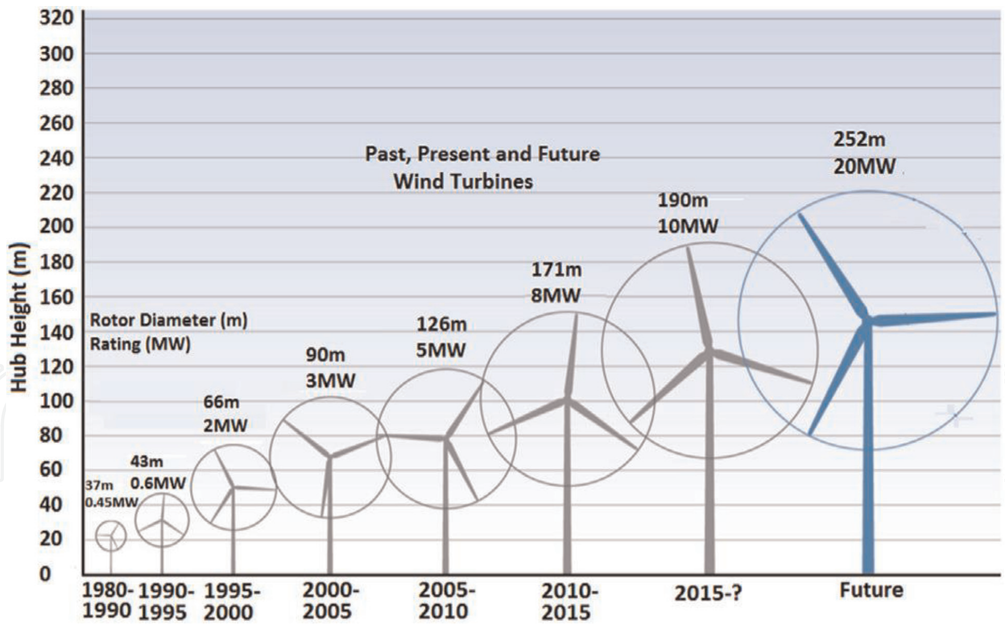

Figure 1.
Growth in size and power of horizontal axis wind turbine [4].

As the most commonly adopted foundation for OWTs, the monopile had been used as the foundation of 2653 OWTs by the end of 2016, which accounts for over 80% [5], due to their ease of design and manufacture in contrast to other foundation types. A typical monopile is composed of a hollow steel cylinder with a diameter typically spanning 4 to 8 m and a slenderness ratio (driving depth over diameter) less than 10 [5]. A special aspect to consider with monopile foundations for OWTs is that the vertical load mainly comprised of gravity load is relatively small compared with other offshore structures like oil and gas platforms. The horizontal loads generated by wind and wave actions, which are of similar magnitude to the gravity loads, are therefore of particular importance for the design [6]. A typical laterally loaded offshore monopile foundation generally behaves rigidly due to their large bending stiffness and low slenderness ratio [7]. The serviceability requirements including lateral deformation and stiffness rather than ultimate lateral resistance tend to govern design due to strict rotational tolerance specifications for monopile foundations [8].

Under the current and/or wave loadings, severe local scour can be generated around a monopile situated in cohesionless sediments. The maximum scour depth is generally predicted to be proportional to the pile diameter, and scour depths of over 1.5 times pile diameter were observed in many practical installations [9]. Considering the lower slenderness ratio compared with more conventional offshore pile for oil and gas industries, the maximum scour depth at a monopile may account for over 25% of the driving length [10]. This scour-induced driving length reduction has significant influence on both quasi-static lateral responses (e.g., ultimate lateral resistance and deformation stiffness) and dynamic responses (e.g. natural frequency) of monopile foundations. Therefore, proper assessments of local scour and its influence on structural responses are essential to the design of monopile foundation for OWTs.

In view of the complexity of local scour phenomenon around a monopile and scour effects on manifold monopile responses, this chapter aims to systematically summarize the predicting methods involving the maximum scour depth and the time scale under various flow conditions. The controlling mechanisms of local scour around a monopile are also revisited. Subsequently, we examine existing research on the effects of local scour on the responses of the monopile foundation.

2. Local scour around a monopile

2.1 General description and scour mechanisms

In the river hydraulics, the local scour at the bridge piers has been widely recognized to be one of the main causes for the structure failure [11]. Hence, the phenomenon of scouring at bridge piers has ever been studied extensively over the past half century from various aspects, including local scour mechanisms associated with flow characteristics, prediction of the maximum scour depth, etc. Comprehensive descriptions of scour around a pile or bridge pier in steady currents have been given in Refs. [12, 13].

For a pile foundation installed in the marine environment, several phenomena with regard to the flow pattern would arise including a horseshoe vortex (HSV, or sometimes necklace vortex due to its shape) in front of the pile, wave vortices convected through the pile's lee-side, and the contraction streamlines at the side edges of the pile. These changes induce an increased sediment transport capacity. If the scouring potential created by the large-scale eddy structures is strong enough to overcome the particles' resistance to motion, local scour will be initiated around the pile (see **Figure 2**). As scour hole develops, the strength of the large-scale eddy structures will gradually be weakened, thereby reducing the transport rate from the local scour region. Equilibrium is reestablished if the sediment inflow of the scour hole is equal to the outflow for live-bed scour, or the shear stress caused by vortices is equal to the critical shear stress of incipient sediment motion at the bottom of the scour hole for clear-water scour. Two major issues concerning the local scouring process, namely the equilibrium scour depth and the time scale, usually need to be quantitatively characterized and are detailed in Sections 2.2 and 2.3, respectively. We herein focus on reexamining the general scouring mechanisms, which mainly involve characterization of the flow pattern under different incoming flow conditions.

A surface-mounted cylinder induces the boundary layer separation from the upstream bed in the incoming flow, resulting in a HSV system at the upstream junction corner of the cylinder. The existing test observations indicated that the HSV (including the down-flow) upstream of a cylinder is the most evident and significant contributor to the scour process in currents alone. Much work has been done for the HSV at a cylinder in steady currents. Many researchers investigated the HSV at a flatbed for the laminar case [14–16]. However, most of the practical HSVs occur with turbulent approach boundary layers [17]. Baker [18] used smoke- and oil-flow visualization to observe the turbulent HSV system. The variation in the

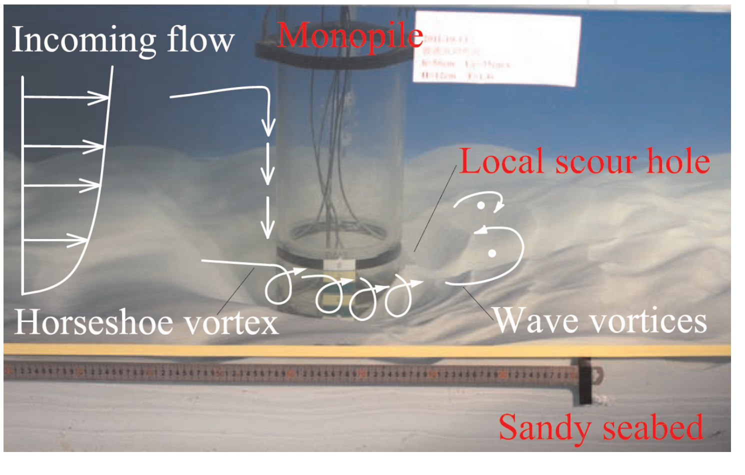

Figure 2.
General flow patterns involving local scour around a monopile.

position of the primary horseshoe vortex with the flow parameters was presented graphically. Dargahi [19] tried to examine the coupling between the flow field and scouring around a circular pile. The consequences of an unsteady vortex pattern were indicated. With the development of the scour hole, the vortex rapidly grows in size and strength as additional fluid attains a downward component and the strength of the down flow increases (see [20]). This conclusion was also verified by the subsequent flow measurements [21, 22].

Kirkil et al. [23] investigated the influence of large-scale coherent structures and macroturbulence events on the scour hole development at a cylinder. The results indicated that the pressure fluctuations and turbulent kinetic energy levels inside the primary necklace vortex were much larger than those associated with the turbulence inside the boundary layer flow approaching the cylinder. Strong ejections and uplift events were observed in the region just behind the cylinder. Recently, the evolution of the HSV in a scour hole around a circular pile was studied by Guan et al. [24] using 2D Particle Image Velocimetry (PIV) technique. The results indicated that the horseshoe vortex system evolves from one initial small vortex to three vortices along the upstream slope of the developing scour hole. Both the strength and size of the main vortex increase with increasing scour hole size. Most existing studies regarding the HSV at a scour hole in steady currents mainly focus on describing the evolution of the HSV itself rather than revealing the time-dependent coupling between the HSV and the scour hole. There is still a great need to improve the understanding of this complex coupling process (see [25]).

In contrast to the substantial amount of accumulated knowledge for HSV in steady currents, relatively fewer studies (e.g., [26]) can be found regarding the flow patterns around a cylinder under waves, although the two-dimensional vortex flow behind a free cylinder subject to an oscillatory flow is well understood (e.g., [27]). Sumer et al. [28] concluded that the scour around a pile in waves is governed by the action of both lee-wake vortices and the horseshoe vortex. Their observations showed that the lee-wake vortices shed from the cylinder act like cyclones, sweeping the sediment grains into its core region and then lifting the grains upward via the updraft in the vortices. The extension and circulation of the lee-wake vortices are governed primarily by the Keulegan Carpenter (*KC*) number [27]. The *KC* number is defined as

$$KC = U_{\mathrm{wm}} T / D \tag{1}$$

where U_{wm} is the maximum velocity of the undisturbed wave-induced oscillatory flow at the sea bottom above the wave boundary layer, D is the pile diameter, and T is the wave period. In contrast to the controlling role of the lee-wake vortices in eroding the sediment grains around a cylinder, the HSV would be less significant because the wave boundary layer is usually thin (see [29, 30]), especially for relatively small *KC* numbers [26]. Regarding monopile foundations for OWTs, the corresponding value of *KC* number is usually low due to the large diameter [31]. Therefore, the effect of the HSV might be insignificant for the scour development around a monopile under waves.

In general, the controlling mechanism of the scour process around pile foundation in wave-alone or in current-alone condition has been well established. Yet for the condition of combined waves and currents, which is a common scenario in marine environments, the physical mechanism for the scouring phenomenon is less understood. When the waves and currents coexist, the sediment is normally picked up by the waves due to its higher capacity of lifting sands and transported by the currents due to its higher capacity of carrying sands. Nevertheless, the effect of waves and currents' coexistence is more than just a superimposition of their capacities of initiating and carrying sediment, due to a nonlinear interaction between waves and currents within and outside the bottom boundary layer [32–34]. The only experimental investigation so far on the flow pattern around a vertical pile in a combined current-wave flow was made by Sumer et al. [26]. Their results showed that introducing the following currents in the waves increases the size and lifespan of the horseshoe vortex and lowers the critical KC number for the threshold of horseshoe vortex. The horseshoe vortex exists for smaller KC with increasing the current-to-wave velocity ratio. This result is related to the increase in the adverse pressure gradient in front of the pile caused by the superimposed currents. For small values of KC (such as $KC \approx O(10)$), the presence of the horseshoe vortex is quite limited in both space and time domain, and its influence on the scour is much less than that in steady currents ($KC \approx \infty$). That is, with decreasing KC, the effect of horseshoe vortex decreases and that of the vortex shedding increases accordingly.

2.2 Equilibrium scour depth

The equilibrium scour depth prediction is a key concern in the geotechnical design for the coastal and offshore foundations. On the basis of laboratory flume tests and field data, many empirical equations have been proposed with respect to the equilibrium scour depth around a cylinder over the past few decades.

For the bridge scour in steady currents, Melville and Sutherland equation [35] and the Colorado State University (CSU) equation [36] are two of the most commonly used scour equations. They give somewhat conservative estimates of scour depth, the former perhaps more so than the latter [37]. Other well-known scour equations were reviewed by Deng and Cai [38]. The accuracy of several most commonly adopted scour equations were evaluated and compared by Johnson [37], Mueller [39] and Sheppard et al. [40], using a large set of field data.

Unlike the pier-scour in bridge waterways, the local scour at offshore monopile foundations should consider the action of waves. For scour depth around pile exposed to waves alone, the number of prediction equation is much fewer compared with that under steady currents. An empirical expression for scour depth at a circular slender pile exposed to regular waves was established [28]:

$$S/D \approx 1.3[1 - \exp(-0.03(KC - 6))] \text{ for } KC \geq 6 \tag{2}$$

where S is the equilibrium scour depth at the pile. Note that Eq. (2) is valid for the live-bed conditions. Sumer et al. [41] further investigated the effect of the soil density on the scour depth at a pile in waves. The scour depth was significantly increased when the bed soil was changed from medium dense sand to dense sand. Dey et al. [42] presented the results of equilibrium scour depths at circular piles in clay and sand-clay mixed beds under waves alone. The variation of equilibrium scour depth with KC for different soil conditions follows an exponential law, as was given in [28], having different coefficients and exponents. Recently, Zanke et al. [43] proposed the following unifying equation for the prediction of equilibrium scour depth around a pile under the action of waves, tidal or steady currents.

$$S/D = 2.5(1–0.5\, U_{cr}/U)\, x_{rel} \tag{3}$$

where $x_{rel} = x_{eff}/(1 + x_{eff})$, $x_{eff} = 0.03(1 - 0.35U_{cr}/U)\ (KC\text{-}6)$, U is the mean velocity in case of steady currents, and U_{cr} is the critical velocity for initiation of sediment motion.

For shallow-water subsea locations, waves often coexist with currents, propagating either following or opposing the currents. This brings the soil response around marine structures more complicated than that due to waves or currents alone. Nevertheless, the related research is relatively few. Sumer and Fredsøe [44] conducted a series of tests of irregular waves propagating either along or perpendicular to the current, indicating that the scour depth for combined waves and currents is influenced by the KC number and the current-to-wave velocity ratio. The current-to-wave velocity ratio is defined as $U_{cw} = U_c/(U_c + U_{wm})$, in which U_c represents the undisturbed near-bed current velocity component of the combined flow, and U_{wm} is the maximum velocity of the undisturbed wave-induced oscillatory flow at the sea bottom above the wave boundary layer. Sumer and Fredsøe [45] carried out re-analyses of scour data in [44] and derived the following empirical expression for the scour depth under combined waves and current:

$$S/D = S_c/D\{1 - \exp[-A(KC - B)]\} \text{ for } KC \geq B \quad (4)$$

in which S_c is the scour depth for the current-only case, and the parameters A and B are given as $A = 0.03 + 0.75U_{cw}^{2.6}$ and $B = 6\exp(-4.7U_{cw})$. The validity range of Eq. (4) is limited to $4 < KC < 25$. The value of S_c/D can be expressed with a mean value $S_c/D = 1.3$ and a standard deviation $\sigma_{S/D} = 0.7$. The maximum scour depth for the live-bed scour regime is suggested to take as $S_c/D = 1.3 + \sigma_{S/D} = 2.0$ or $S_c/D = 1.3 + 2\sigma_{S/D} = 2.7$ for design purpose. The large variation range of S_c/D in Eq. (4) could produce a great arbitrariness and uncertainty in the practical engineering application. Moreover, the accuracy of Eq. (4) is not very much optimistic [46]. Rudolph and Bos [47] carried out model tests on scour around a monopile under combined waves and currents with oblique directions, focusing on the range $1 < KC < 10$. They proposed an improved scour depth prediction formula based on Sumer and Fredsøe [45] by analyzing their new data and preceding data.

Recently, Qi and Gao [31, 48] conducted an experimental investigation of the local scour development under combined waves and currents at a monopile. The influence of the wave propagating direction relative to currents is obvious. The experimental results indicated that the wave-current interaction had a substantial effect on the time-development of local scour and the resulting equilibrium scour depth. An average-velocity-based Froude number (Fr_a) was proposed to correlate with the equilibrium scour depth (S/D) at offshore monopile foundation in combined waves and currents [48]. The definition of Fr_a is

$$Fr_a = U_a/\sqrt{gD} \quad (5)$$

in which U_a $\left(= \frac{1}{T/4}\int_0^{T/4} (U_c + U_{wm}\sin(2\pi t/T))dt = U_c + \frac{2}{\pi}U_{wm}\right)$ is the average water particle velocity during one-quarter cycle of oscillation under combined waves and currents, when the oscillatory motion and the currents are in the same direction; t is the time and g denotes the gravitational acceleration. The equilibrium scour depths (live-bed scour regime) under combined waves and currents obtained from the experiments were plotted as a function of Fr_a (see **Figure 3a**), along with those of in [44, 49]. Following empirical expression for the correlation between S/D and Fr_a was given for predicting equilibrium scour depth under live-bed conditions.

$$\lg(S/D) = -0.8\exp(0.14/Fr_a) + 1.11 \; (0.1 < Fr_a < 1.1, 0.4 < KC < 26) \quad (6)$$

Eq. (6) indicates that the scour depth approaches its mathematical asymptotic value ($S/D \approx 2.0$) as Fr_a increases (e.g., larger than 1.0). Note that this asymptotic value is in the range of a typical scour depth prediction ($S/D \approx 1.7$–2.4) by previous local scour equations around a pile for current-alone conditions. The prediction

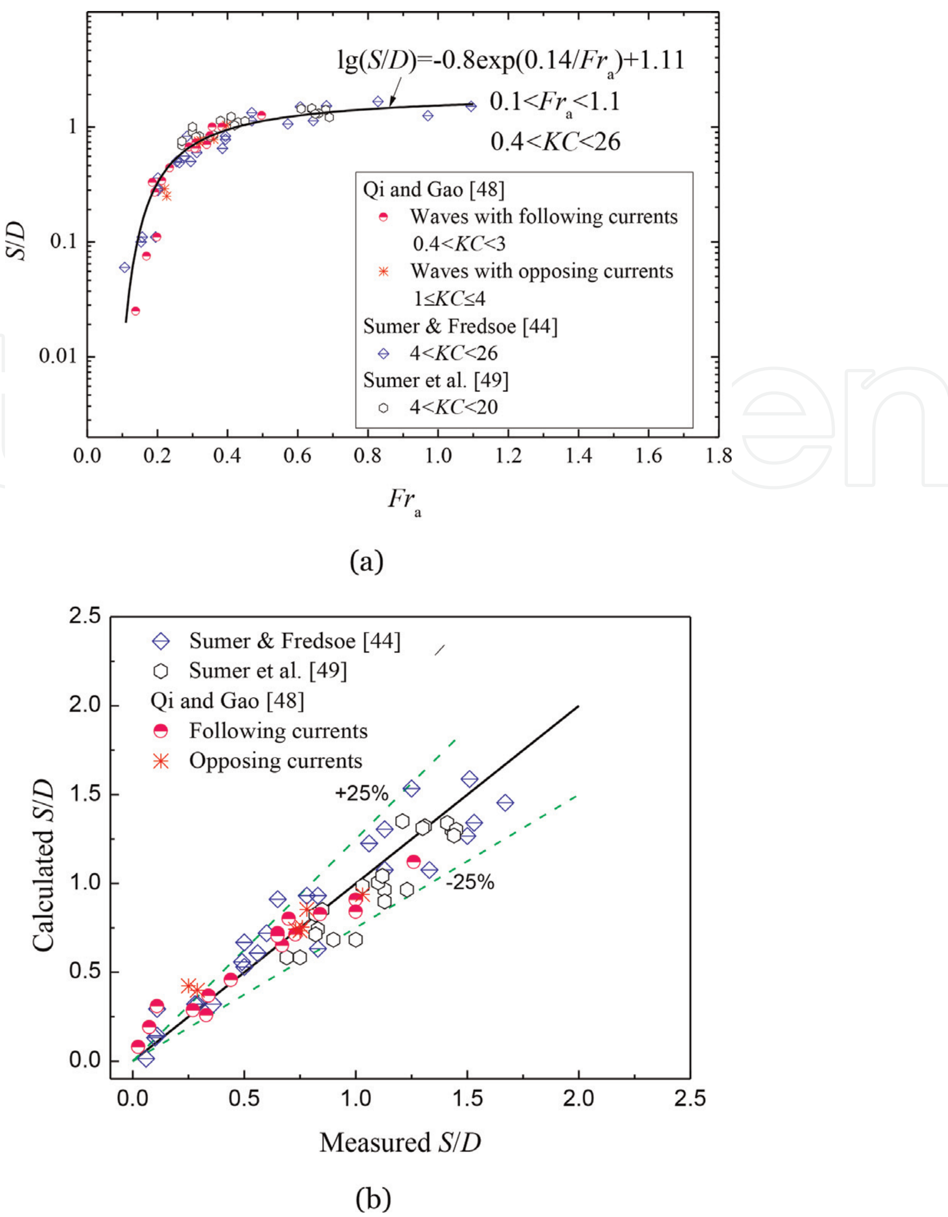

Figure 3.
(a) S/D vs. Fr_a for combined waves and currents; (b) comparison of measured and predicted scour depths [48].

using the empirical correlation generally distributes in the range of 25% error lines (see **Figure 3b**), which is superior to the existing formula.

As aforementioned, most existing equations for predicting the equilibrium scour depth around a cylinder are based predominantly on scaled laboratory flume data. Therefore, the inherent scaling issue is worthy of clarifying before extrapolating the results of small scale scour experiments to prototype [50]. The scale effect is essentially attributable to the use of three independent length scales in local scour experiments: cylinder diameter, sediment size, and water depth [51]. The three length scales lead to several controlling similarity parameters that inevitably cannot be satisfied concurrently. Two aspects are specifically drawing attention involving the scale effect: one associated with inadequate similitude of large scale turbulence generated around a cylinder during scour tests and the other with the distortion of sediment size scaling.

The similitude of large scale turbulence requires preservation of flow patterns so that pressure heads along flow path scale directly with the geometric scale relating the small cylinder in a flume test to a prototype pile. The Froude number defined with incoming flow velocity and pile diameter is proved useful for reflecting the similitude associated with flow-field [51, 52]. It was concluded that the flume-based equations for predicting equilibrium scour depth at a cylinder may not adequately account for the similitude of large scale turbulence and thus commonly lead to over-conservative estimations in prototype applications [51].

Most flume experiments were forced to use particles of comparable size to full-scale particles due to requirements of both the similitude associated with particle mobility and the natural size limit to which bed particles become cohesive. As such, the similarity of sediment size with respect to pile diameter cannot be maintained. According to Melville and Chiew [53], D/d_{50} barely has effect on the scour development for $D/d_{50} > 50$, with d_{50} as the median grain size of the sediment. However, some more recent research indicates a decrease in S/D at very large values of D/d_{50} [54, 55]. Consequently, a prototype scour depth prediction based on the flume scour data is greater than that in the field, that is, a relatively conservative or safe prediction. A comparison between the maximum calculated scour data from different formulations used in standard and technical recommendations for the design of offshore wind farms and available scour data in European wind farms found in technical reports was once conducted by Matutano et al. [9]. The observed maximum scour depths were largely less than estimated in most offshore wind farms studied, which is consistent with the similarity analysis.

It should be noted that various offshore standards like DNV·GL [8] recommend Eq. (2) proposed in [26] to estimate the scour depth around monopile foundations for the OWTs under combined waves and currents. This could be inappropriate and potentially lead to great inaccuracies [56].

2.3 Time scale

The time scale of scour process (T_0) is a certain amount of elapsed time for a substantial amount of scour to develop [45], which is essential for predicting the scour depth at any instant in a certain wave and/or current condition. In the case of live-bed scour, the equilibrium scour depth is achieved faster than the clear-water case, generating a smaller time scale. The time scale of scour process can be defined in several ways according to different mathematical functions for approximating the scour development toward the equilibrium stage [57]. For example, Briaud et al. [58] proposed a hyperbolic function $S_t = S_e\left(\frac{t}{t+T_0}\right)$, where S_e is the equilibrium scour depth. Alternatively, a more commonly used definition was proposed in [59]: $S_t = S_e\left(1 - \exp\left(-\frac{t}{T_0}\right)\right)$. The value of the time scale can be obtained by fitting the measured scour depth development curve with these functions of S_t. The normalized time scale is usually defined as

$$T^* = T_0 \frac{\left(g(s-1)d_{50}^3\right)^{\frac{1}{2}}}{D^2} \tag{7}$$

where s is the specific gravity of sand grains.

For steady currents, the normalized time scale is associated with the ratio of boundary layer thickness to pile diameter (δ/D) and the Shields parameter (θ), using following empirical expression for live-bed scour regime [59].

$$T^* = \frac{1}{2000}\frac{\delta}{D}\theta^{-2.2} \tag{8}$$

The Shields parameter (θ) is defined as

$$\theta = \frac{U_f^2}{g(\rho_s/\rho_w - 1)d_{50}} \tag{9}$$

in which U_f is the maximum value of the undisturbed friction velocity, ρ_s is the sediment grain density, and ρ_w is the water density. The detailed calculation procedure of θ is given by Soulsby [60].

In the case of waves, the time scale of the scour process around a cylinder is governed by two parameters, namely the *KC* number and the Shields parameter. The empirical expression of T^* based on *KC* and θ for live-bed scour regime can be represented by [59].

$$T^* = 10^{-6}\left(\frac{KC}{\theta}\right)^3 \tag{10}$$

Under combined waves and currents, Petersen et al. [61] concluded that the time scale of scour varies with the *KC* number, the Shields parameter associated with the wave component of the flow (θ_w), and U_{cw}. The time scale of scour increases significantly when even a slight current is superimposing on a wave. On the basis of the data of Refs. [61, 62] and their own, Chen and Li [63] proposed a piecewise fitting formula for the time scale of scour under combined waves and currents (see **Figure 4**)

$$T_0{}^* = \begin{cases} 8.67 \times 10^{-5}\theta_w^{-5.15}U_{cw}^{28.1(0.152-\theta)} & \text{for } 0.3 < U_{cw} < 0.44 \\ 1.35 \times 10^{-4}\theta_w^{-2.2}U_{cw}^{-6.8} & \text{for } 0.44 \le U_{cw} \le 0.7 \end{cases} \tag{11}$$

2.4 Backfilling process

Backfilling process is the deposition of sediment into a scour hole previously generated, when the pile is exposed to a changing flow environment (the flow

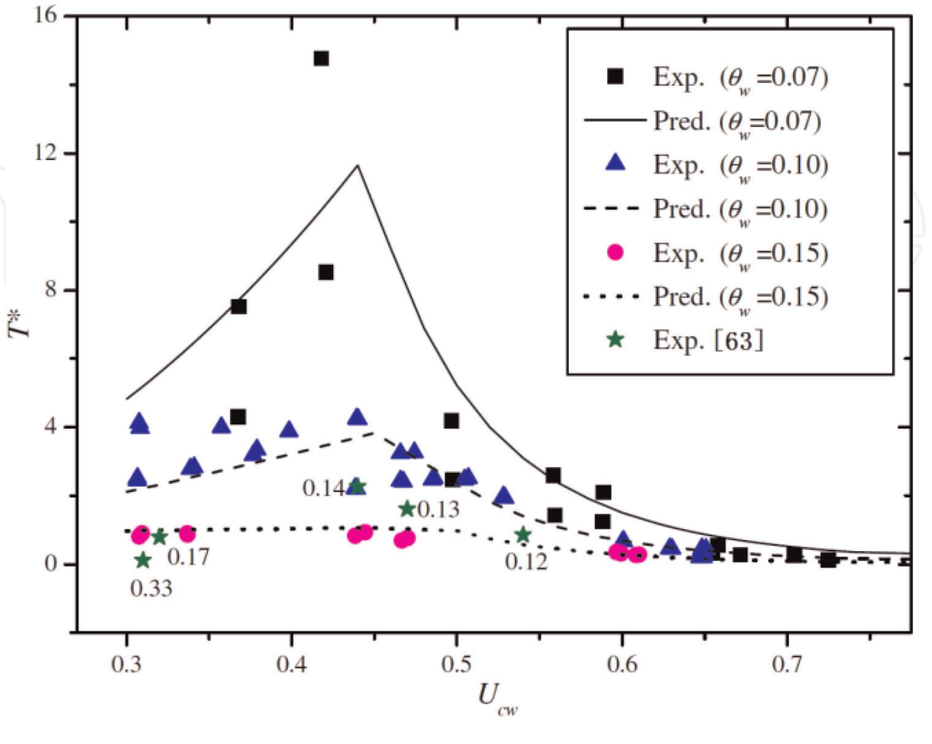

Figure 4.
Comparison of predictions using Eq. (11) and calculated results of normalized time scale based on observed data under combined wave-current conditions [63].

environment changing from, e.g., a steady current to a wave, from a steady current to combined waves and currents, or from a wave to a smaller wave). For the monopile foundations of the OWTs, the flow climate changes continuously, hence leading to scour and backfilling in an alternating fashion. The backfilling process needs to be quantitatively estimated to establish models for predicting the time history of scour and backfilling for large periods of time (see [64]).

Hartvig et al. [65] experimentally studied the scour and backfilling around a pile subjected to alternating sequences of currents with and without superimposed irregular waves. The results indicated that initially current-scoured beds, when subjected to waves, are backfilled about 10 times slower than the scoured ones. Sumer et al. [49] later presented a systematic investigation of the scour holes backfilling under waves or combined waves and currents around a pile. The results showed that the scour depth corresponding to the equilibrium state of backfilling is the same as that corresponding to the equilibrium state of scour around the pile for the same wave or combined waves and currents climate. That is, the final equilibrium scour is uninfluenced by the loading history of the flow but only dependent on the flow condition at the last stage if the last loading stage is sufficiently long. The time scale of backfilling is much larger than that of scour when the KC number associated with the backfilling is $KC < O(10)$ (typical wind farm application). Various empirical equations involving the time scale were further proposed for different flow environment changes.

Backfilling can reduce the scale of the scour hole, which is beneficial to the bearing behavior of a monopile unprotected against scour. Sørensen et al. [66] assessed the relative density of the backfilled soil around a model monopile of 0.55 m diameter based on the test in a large wave channel. The relative density of the backfill material was found to be rather large, varying between 65 and 80%. Note that these values were obtained from only one set of laboratory tests, and lower densities may exist. The backfilled soil was found to increase the soil support to a monopile foundation significantly. Therefore, an optimized design with respect to both the fatigue limit state and the ultimate limit state can be achieved by considering the time variation of the scour depth [67].

3. Effects of local scour on the lateral response of a monopile

3.1 Lateral bearing behavior

The lateral response of a pile is commonly evaluated using a load transfer approach, with "*p-y*" curves quantifying the nonlinear interaction between the pile and the surrounding soil. The *p-y* curves idealize the soil as a series of independent springs distributed along the pile length, with each spring describing the nonlinear relationship between the lateral soil resistance (p) and the lateral deflection of the pile (y). Various formulations for *p-y* curves have been developed for sands, for example Refs. [68–71]. The results in Refs. [68, 69] form the basis of the widely used API method [72].

Scour around submarine structures leads to a reduction in the effective stresses and hence strength and stiffness of the soil at a given depth around a pile. As scour depth is predicted to scale with the pile diameter, scouring can impact greatly on the overall response of large-diameter monopiles due to the low slenderness ratio (typically between about 3 and 10). As shown in **Figure 5**, scour reduces the pile embedment depth from L to L' and increases the load eccentricity (cantilever length) from e to e', changing the profiles of lateral soil resistance p, inducing much larger deformations of the pile and reducing the foundations stiffness.

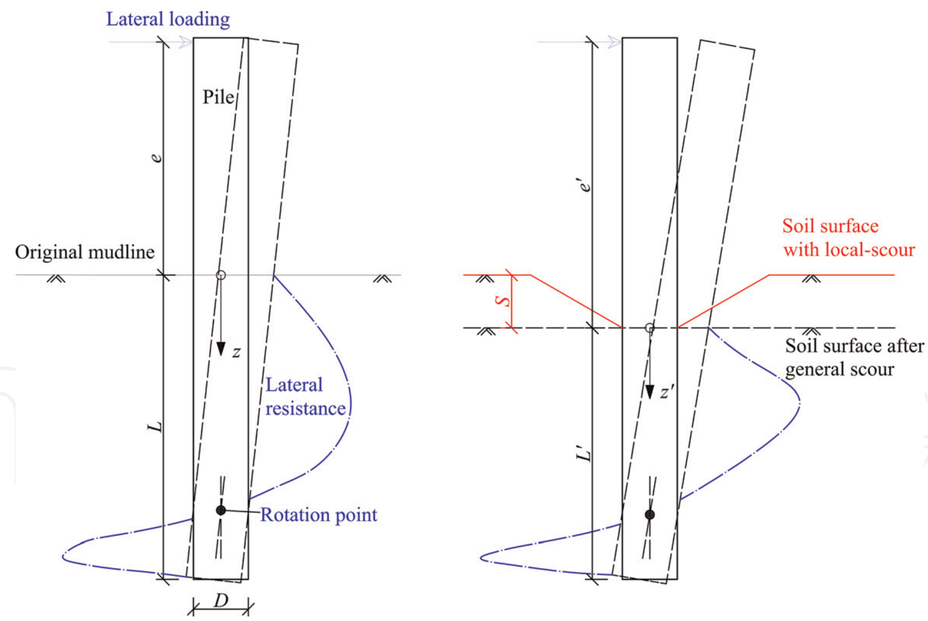

Figure 5.
Illustration of scour effect on the lateral response of a shallowly embedded pile [73].

Scour can cause the *p-y* response at a given absolute depth z (measured from the original soil surface or "mudline") to soften, reducing both initial stiffness and the limiting resistance. In design codes such as DNV·GL [8], local scour is often considered to cause complete loss of soil resistance down to the depth of scour below the original seabed while estimating the pile capacities. Although such a design practice is simple, it often leads to extreme conservative pile foundation design and subsequent unnecessary cost [73]. In recent years, the importance of scour hole dimensions for pile capacities has been increasingly recognized.

In an analytical study [74], general scour effects were incorporated by updating the parameters per unit length (p_{ult}) at a given depth to account for the overconsolidation induced by removal of a scour depth of sand. Lin et al. [75] and Yang et al. [76] further modified the ultimate lateral resistance due to changes in the shallow wedge-type failure mechanism to consider the effects of the local scour. Results indicated that the local scour hole would result in much higher lateral soil resistance for a given depth than for the general scour case, that is, complete removal of the soil surface layer. Tseng et al. [77] combined the approach of Sørensen [78] for modifying the initial modulus of subgrade reaction (k_{py}) and the approach of Lin et al. [75] for modifying p_{ult} to evaluate the scour effect on the deformation response of monopile foundations. According to the case analysis, when the *p-y* curve method suggested by the design guidelines for an offshore wind turbine was used to design the monopile foundation for an OWT, the foundation deformation was underestimated for a scour depth of less than pile diameter, and foundation stiffness was underestimated for a scour depth of greater than pile diameter.

A series of centrifuge tests were conducted by Qi et al. [73] to investigate the scour effects on *p-y* curves. A practical approach to incorporate effects of scour on the *p-y* curves was proposed by adopting an effective soil depth (z_{e}) in the determination of *p-y* curves. The effective soil depth was expressed by

$$\frac{z_{\text{e}}}{D} = \frac{z'}{D} + \tanh\left(f\frac{z'}{D}\right)\frac{S}{D} \qquad \begin{cases} f \approx 1.5 & \text{for local-scour} \\ f = 0 & \text{for general-scour} \end{cases} \tag{12}$$

where the effective soil depth z_{e} is a weighted-average of the soil depth relative to the original mudline z and the soil depth below the current scour base z' $(= z - S,$

S is the scour depth), f is an empirical parameter indicating the transition rate for the effective soil depth from $z_e = z'$ at the current mudline to $z_e \approx z$ as the soil depth increases. The recommended value of $f = 1.5$ for local-scour conditions was based on the tests with 30° slope angle of the scour hole. As the slope angle of the scour hole decreases, the effect of the sloping overburden soil above the level of the scour base reduces and the value of f should be reduced accordingly. This conclusion conforms to the results of a recent study by Lin and Wu [79].

Local scour not only exaggerates the deformation and reduces the stiffness of the monopile foundation, but also changes its bearing mechanism. Monopile foundations for the OWTs generally behave rigidly, rotating as a whole and developing a "toe-kick" phenomenon. **Figure 6** illustrates the mobilized soil resistance components of a laterally loaded short pile. Significant base shear and axial resistance will be mobilized at the pile tip if the slenderness ratio gets sufficiently small. Moreover, vertical side resistances emerge around the pile shaft due to the mobilized horizontal displacement of the pile tip and rotation of the pile. Numerical investigations by Bekken [80] and Byrne et al. [81] have confirmed the significant contributions due to the horizontal pile tip displacement and rotation of the pile on the resistance of a monopile.

To investigate the scour effect on the behavior of a laterally loaded monopile, a three-dimensional finite element model was proposed and verified by Qi and Gao [83]. The results indicated that the scour could induce a significant transition of pile behavior for a typical monopile foundation of the OWTs. **Figure 7(a)** shows the variation of y_p/y_n with E_sL^4/E_pI_p, in which y_n denotes the lateral pile displacement at the loading position obtained from the 3D finite element results, and y_p denotes the lateral pile displacement according to the conventional p-y method. The non-dimensional expression of E_sL^4/E_pI_p is aimed to reflect the rigidity of the pile foundation [7, 84], where I_p denotes the second moment of area of a pile and E_pI_p

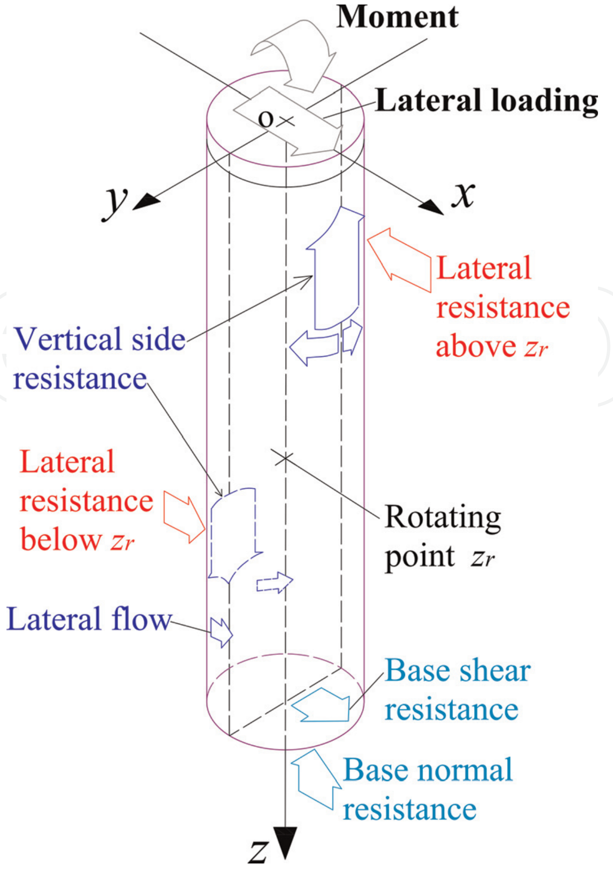

Figure 6.
Resistance components of a laterally loaded monopile foundation [82].

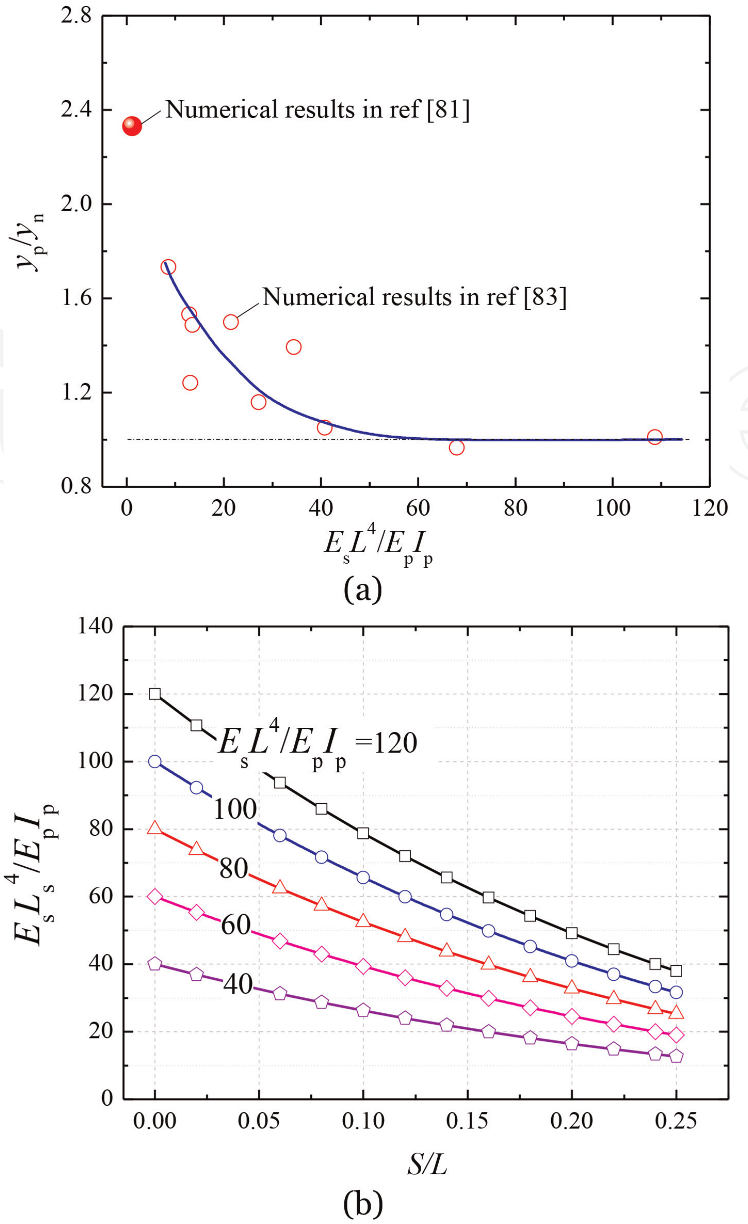

Figure 7.
(a) Variation of y_p/y_n with E_sL^4/E_pI_p; (b) effect of scour depth normalized with pile embedment depth S/L on $E_sL_s^4/E_pI_p$ [83].

represents the bending stiffness of the pile. It is seen that for an approximate range of $E_sL^4/E_pI_p > 50$, the value of y_p/y_n is generally equal to 1.0, while the value of y_p/y_n obviously deviates from the value of $y_p/y_n = 1.0$ for $E_sL^4/E_pI_p < 50$. The deviation of y_p/y_n implies that due to the scour-induced increase of pile rigidity (see **Figure 7(b)**), the pile's tip and shaft resistance could become a significant component of the whole soil resistance. The parameter L_s in **Figure 7(b)** denotes the pile embedment depth after scour. The traditional *p-y* approach only takes account of the lateral soil resistance and thus the scour would render the traditional *p-y* approach inapplicable for post-scour conditions.

There are relatively fewer studies concerning the scour effect on the pile behavior under cyclic loading compared with aforementioned studies on the monotonic pile behavior [85]. Achmus et al. [86] numerically quantified the scour-induced increase of pile deformation by adopting a degradation stiffness model to account for cyclic loading. The results indicated an evident accumulation of lateral deformation under cyclic loading. Up to now, no systematic investigations into the influence of scour on the cyclic pile behavior can be found in the literatures. This issue needs to be further studied. Moreover, local scour and backfilling occurs around a monopile foundation in an alternating fashion due to the continuously changing flow climate in marine conditions. This variation of scour depth should also be included while evaluating the long-term cyclic pile behavior.

3.2 Natural frequency and fatigue life (FL)

Compared to other types of OWT foundations such as gravity base, tripod, and suction bucket, the monopile is a dynamically sensitive structure due to its flexibility. The primary excitation forces arise from the wind, waves, and the rotor excitations. The fundamental frequency f_0 (the first tower bending frequency) of the structure is the most important controlling parameter for its dynamic response.

The OWTs are usually designed as soft-stiff structures in order to avoid resonances, meaning that f_0 is above the rotational frequency of the rotor f_{1P} but below the blade-passing frequency f_{3P} (see **Figure 8**). The excitation frequencies related to environmental loads from wind and waves are typically below the 1P frequency for OWTs with relatively small installed capacities, for example, smaller than 3.6 MW [87, 88]. Nevertheless, for a 6–8 MW modern OWT on a monopile, designed for the soft-stiff frequency range, f_0 would be around 0.20–0.23 Hz [89]. In this frequency range, the fundamental mode of the structure would resonate with the waves at low wind speeds and be exposed to high spectral energy of waves during higher wind speeds. Due to the narrow soft-stiff frequency range for the OWTs on monopile foundations, even a small natural frequency shift from the initial design value may finally lead to resonance and the resulting stress in the materials of the monopile will be higher than in the quasi-static case. This high stress would potentially reduce the FL of the OWTs significantly.

Scour around the monopile leads to significant reduction of f_0. This would make f_0 align with the frequency of the passing sea waves or the rotational frequency of the rotor (f_{1p}) under certain circumstances, exposing structures to the threat of resonances. Sørensen and Ibsen [67] calculated the undamped natural frequencies of an existing offshore wind farm at HornsRev1 by means of the Winkler model approach. The stiffness derived from *p-y* curves given in the API code was adopted in their desk study, without accounting for the degradation of stiffness due to cyclic loading. The results revealed that the first natural frequency decreases with approximately 5% when the scour depth reached 1.3*D*. Prendergast et al. [90] conducted finite element numerical modeling to examine the scour effects on the natural frequency of a 3.6 MW OWT on a monopile in typical offshore sand deposits. The numerical model was validated by scale model tests and proved capable of tracking the scour-induced change in the natural frequency of the system. A reduction of up to 8.5% in natural frequency was observed in loose sand for

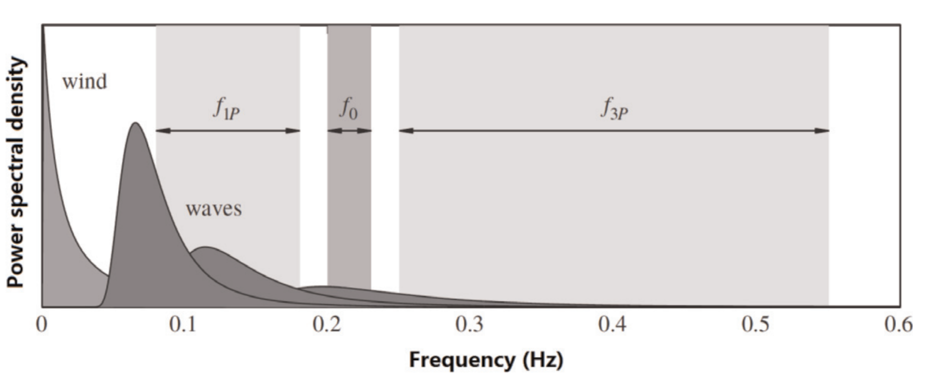

Figure 8.
Illustration of typical excitation ranges of a modern 6–8 MW OWT. Wave spectra represent different wind speeds. Not in scale [89].

S/*D* = 1.3. A comparison among cases with different soil stiffness profiles suggests that scour-induced resonance of an OWT on a monopile is most likely to occur in loose deposits. Prendergast et al. [91] recently improved the numerical model to further include the effect of spatial variability in soil properties derived from measured Cone Penetration Test (CPT) data. A stochastic ground model was developed to account for the uncertainty in soil-structure interaction stiffness for a given offshore site. The results indicated that the first natural system frequency reduces while the range of predicted system frequencies increases as the scour progresses. This means that the results of frequency-based SHM (structural health monitoring) technique for assessing scour magnitude-based solely on first natural frequency measurements becomes less certain for a deeper scour hole.

Several recent studies have focused on the scour effects associated with the FL of OWTs. Damgaard et al. [92] performed fully coupled aero-hydro-elastic simulations to evaluate the scour effects on the fatigue loads for parked OWTs. It was shown that a scour hole of 1.3*D* deep increases the fatigue damage equivalent moment with approximately 40%. Note that time-varying stiffness/damping properties of the soil due to long-term cyclic loading [93, 94] and scour depth variation due to backfilling are not accounted for. Rezaei et al. [95] presented a study of scour and backfilling effects on the FL of a 5 MW monopile supported OWT, using quasi-static, modal, and time-domain fatigue analyses. It was demonstrated that a scour depth of 1.5*D* could result in a 45% reduction of the FL of the wind turbine structure. Backfilling is beneficial to extend FL of the OWTs. Nevertheless, the relative density barely has effect on the FL of the OWTs.

4. Concluding remarks

Monopile is the most commonly adopted foundation type for OWTs. Local scour induced by waves and/or currents can jeopardize the function of the structure system to a great extent. In contrast to bridge scour which has been sufficiently studied over the past half century, an important feature of scour phenomenon around an offshore monopile stems from the various flow conditions in a marine environment, namely waves only, currents only, and combined waves and currents. In view of the complexity of incoming flow conditions, several crucial aspects related to local scour around a monopile foundation are reviewed, including the fundamental scour mechanisms, the maximum scour depth, the time scale, and the backfilling process. The inherent scaling issue arising from extrapolating the results of small scale scour experiments to prototype is clarified.

The driving depth of an offshore monopile can be significantly reduced by the local scour due to the low slenderness ratio, consequently imposing great influence on twofold structural responses. First, scour will cause the *p-y* response at a given absolute depth to soften, reducing both initial stiffness and the limiting resistance. Moreover, scour would render the traditional *p-y* approach inapplicable for post-scour conditions due to the change of bearing mechanism. Second, scour around the monopile leads to significant reduction of the fundamental frequency. This would make the fundamental frequency align with the frequency of the passing sea waves or the rotational frequency of the rotor under certain circumstances, exposing structures to the threat of resonances.

The current upward trends in both water depth and size of OWTs have led to consequential growth mainly in the horizontal loading. Monopiles with diameters up to 10 m have been proposed as a feasible option to support the OWTs with approximately 10 MW installed capacity. To efficiently minimize the cost while remaining safety, more meticulous considerations for monopile design are in need involving the scour depth prediction and evaluation of scour effects on structural responses. An alternative hybrid foundation system comprising a monopile and a bearing plate (or skirted footing) has been demonstrated to enhance the lateral bearing capacity compared with a monopile [96–99]. Nevertheless, the enhanced capacity of the hybrid foundation largely relies on the proper interaction between the bearing plate and the soils at the shallow zone of the seabed, where local scour and wave-induced pore pressure could occur [100–108]. The extent of local scour and scour effects on both the bearing capacity and natural frequency of a hybrid monopile need to be further investigated.

Acknowledgements

This work is financially supported by the National Natural Science Foundation of China (Grant Nos. 11602273; 11825205) and the Youth Innovation Promotion Association of the Chinese Academy of Sciences (Grant No. 2012014).

Author details

Wen-Gang Qi and Fu-Ping Gao*
Key Laboratory for Mechanics in Fluid Solid Coupling Systems, Institute of Mechanics, Chinese Academy of Sciences, Beijing, China

*Address all correspondence to: fpgao@imech.ac.cn

References

[1] GWEC. Global Wind Report 2016. 8th National Renewable Energy Forum. Ulaanbaatar, Mongolia: Global Wind Energy Council; 2017

[2] Perveen R, Kishor N, Mohanty SR. Off-shore wind farm development: present status and challenges. Renewable and Sustainable Energy Reviews. 2014;**29**:780-792. DOI: 10.1016/j.rser.2013.08.108

[3] Wu XN, Hu Y, Li Y, Yang J, et al. Foundations of offshore wind turbines: A review. Renewable and Sustainable Energy Reviews. 2019;**104**:379-393. DOI: 10.1016/j.rser.2019.01.012

[4] Igwemezie V, Mehmanparast A, Kolios A. Current trend in offshore wind energy sector and material requirements for fatigue resistance improvement in large wind turbine support structures—A review. Renewable and Sustainable Energy Reviews. 2019;**101**:181-196. DOI: 10.1016/j.rser.2018.11.002

[5] Negro V, López-Gutiérrez JS, Esteban MD, Alberdi P, Imaz M, José-María S. Monopiles in offshore wind: preliminary estimate of main dimensions. Ocean Engineering. 2017; **133**:253-261. DOI: 10.1016/j.oceaneng.2017.02.011

[6] Kuo YS, Achmus M, Abdel-Rahman K. Minimum embedded length of cyclic horizontally loaded monopiles. Journal of Geotechnical and Geoenvironmental Engineering. 2012;**138**(3):357-363. DOI: 10.1061/(ASCE)GT.1943-5606.0000602

[7] LeBlanc C, Houlsby GT, Byrne BW. Response of stiff piles in sand to long-term cyclic lateral loading. Géotechnique. 2010;**60**(2):79-90. DOI: 10.1680/geot.7.00196

[8] DNV·GL. DNV-OS-J101: Design of Offshore Wind Turbine Structures. 2013

[9] Matutano C, Negro V, JS L–G, et al. Scour prediction and scour protections in offshore wind farms. Renewable Energy. 2013;**57/**:358-365. DOI: 10.1016/j.renene.2013.01.048

[10] Sørensen SPH, Ibsen LB, Frigaard P. Experimental evaluation of backfill in scour holes around offshore monopoles. In: Frontiers in Offshore Geotechnics II. London, UK: Taylor & Francis Group; 2011. pp. 617-622

[11] Melville BW, Coleman SE. Bridge Scour. CO, USA: Water Resources Publications; 2000

[12] Hoffmans GJCM, Verheij HJ. Scour Manual. Rotterdam: A.A. Balkema; 1997

[13] Whitehouse R. Scour at Marine Structures: A Manual for Practical Applications. London: Thomas Telford; 1998

[14] Baker CJ. The laminar horseshoe vortex. Journal of Fluid Mechanics. 1979;**95**(2):347-367. DOI: 10.1017/S0022112079001506

[15] Seal CV, Smith CR, Rockwell D. Dynamics of the vorticity distribution in endwall junctions. AIAA Journal. 1997;**35**(6):1041-1047. DOI: 10.2514/2.192

[16] Bo H, Hua Z, Younis MY, Yan L, Raza MS. Experimental investigation on the transition of separation/attachment in steady laminar juncture flows. Experiments in Fluids. 2015;**56**(4):1-9. DOI: 10.1007/s00348-015-1943-5

[17] Simpson RL. Junction flows. Annual Review of Fluid Mechanics. 2001; **33**(33):415-443

[18] Baker CJ. The turbulent horseshoe vortex. Journal of Wind Engineering and Industrial Aerodynamics. 1980;**6**

(1–2):9-23. DOI: 10.1016/0167-6105(80)90018-5

[19] Dargahi B. Controlling mechanism of local scouring. Journal of Hydraulic Engineering. 1990;**116**(10):1197-1214. DOI: 10.1061/(ASCE)0733-9429(1990)116:10(1197)

[20] Breusers H, Nicollett G, Shen H. Local scour around cylindrical piers. Journal of Hydraulic Research. 1977;**15**:211-252. DOI: 10.1080/00221687709499645

[21] Dey S, Raikar RV. Characteristics of horseshoe vortex in developing scour holes at piers. Journal of Hydraulic Engineering. 2007;**133**(4):399-413. DOI: 10.1061/(ASCE)0733-9429(2007)133:4(399)

[22] Unger J, Hager WH. Down-flow and horseshoe vortex characteristics of sediment embedded bridge piers. Experiments in Fluids. 2007;**42**(1):1-19. DOI: 10.1007/s00348-006-0209-7

[23] Kirkil G, Constantinescu SG, Ettema R. Coherent structures in the flow field around a circular cylinder with scour hole. Journal of Hydraulic Engineering. 2008;**134**(5):572-587. DOI: 10.1061/(ASCE)0733-9429(2008)134:5(572)

[24] Guan DW, Chiew YM, Wei MX. Characterization of horseshoe vortex in a developing scour hole at a cylindrical bridge pier. International Journal of Sediment Research. 2019;**34**(2):118-124. DOI: 10.1016/j.ijsrc.2018.07.001

[25] Ettema R, Constantinescu G, Melville BW. Flow-field complexity and design estimation of pier-scour depth: Sixty years since Laursen and Toch. Journal of Hydraulic Engineering. 2017;**143**(9):03117006. DOI: 10.1061/(ASCE)HY.1943-7900.0001330

[26] Sumer BM, Christiansen N, Fredsøe J. Horseshoe vortex and vortex shedding around a vertical wall-mounted cylinder exposed to waves. Journal of Fluid Mechanics. 1997;**332**:41-70. DOI: 10.1017/S0022112096003898

[27] Williamson CHK. Sinusoidal flow relative to circular cylinders. Journal of Fluid Mechanics. 1985;**155**:141-174. DOI: 10.1017/S0022112085001756

[28] Sumer BM, Fredsøe J, Christiansen N. Scour around a vertical pile in waves. Journal of Waterway, Port, Coastal, and Ocean Engineering. 1992;**118**(1):15-31. DOI: 10.1061/(ASCE)0733-950X(1992)118:1(15)

[29] Jonsson IG. Wave boundary layers and friction factors. In: Proceedings of the Tenth Conference on Coastal Engineering - American Society of Civil Engineers; 1966. pp. 127-148. DOI: 10.1061/9780872620087.010

[30] Baykal C, Sumer BM, Fuhrman DR, Jacobsen NG, Fredsøe J. Numerical simulation of scour and backfilling processes around a circular pile in waves. Coastal Engineering. 2017;**122**:87-107. DOI: 10.1016/j.coastaleng.2017.01.004

[31] Qi WG, Gao FP. Physical modeling of local scour development around a large-diameter monopile in combined waves and current. Coastal Engineering. 2014;**83**:72-81. DOI: 10.1016/j.coastaleng.2013.10.007

[32] Kemp PH, Simons RR. The interaction between waves and a turbulent current: Waves propagating with the current. Journal of Fluid Mechanics. 1982;**116**:227-250. DOI: 10.1017/S0022112082000445

[33] Kemp PH, Simons RR. The interaction between waves and a turbulent current: Waves propagating against the current. Journal of Fluid Mechanics. 1983;**130**:73-89. DOI: 10.1017/S0022112083000981

[34] Olabarrieta M, Medina R, Castanedo S. Effects of wave-current interaction on the current profile. Coastal Engineering. 2010;**57**:643-655. DOI: 10.1016/j.coastaleng.2010.02.003

[35] Melville BW, Sutherland AJ. Design method for local scour at bridge piers. Journal of Hydraulic Engineering. 1988; **114**(10):1210-1226. DOI: 10.1061/(ASCE)0733-9429(1988)114:10(1210)

[36] Richardson EV, Davis SR. Evaluating scour at bridges. In: Hydraulic Engineering Circular No. 18. 4th ed. U.S. Fed. Hwy. Admin., U.S. Dept. of Transp., FHWA–NHI–01–001; 2001

[37] Johnson PA. Comparison of pier-scour equations using field data. Journal of Hydraulic Engineering. 1995;**121**(8): 626-629. DOI: 10.1061/(ASCE)0733-9429(1995)121:8(626)

[38] Deng L, Cai CS. Bridge scour: Prediction, modeling, monitoring, and countermeasures. Practice Periodical on Structural Design and Construction. 2009;**15**(2):125-134. DOI: 10.1061/(ASCE)SC.1943-5576.0000041

[39] Mueller DS. Local scour at bridge piers in nonuniform sediment under dynamic conditions [PhD thesis]. Colorado: Colorado State University; 1996

[40] Sheppard DM, Melville B, Demir H. Evaluation of existing equations for local scour at bridge piers. Journal of Hydraulic Engineering. 2013;**140**(1): 14-23. DOI: 10.1061/(ASCE)HY.1943-7900.0000800

[41] Sumer BM, Hatipoglu F, Fredsøe J. Wave scour around a pile in sand, medium dense, and dense silt. Journal of Waterway, Port, Coastal, and Ocean Engineering. 2007;**133**(1):14-27. DOI: 10.1061/(ASCE)0733-950X(2007)133:1(14)

[42] Dey S, Helkjær A, Mutlu Sumer B, et al. Scour at vertical piles in sand-clay mixtures under waves. Journal of Waterway, Port, Coastal, and Ocean Engineering. 2011;**137**(6):324-331. DOI: 10.1061/(ASCE)WW.1943-5460.0000095

[43] Zanke UCE, Hsu TW, Roland A, Oscar L, Reda D. Equilibrium scour depths around piles in noncohesive sediments under currents and waves. Coastal Engineering. 2011;**58**:986-991. DOI: 10.1016/j.coastaleng.2011.05.011

[44] Sumer BM, Fredsøe J. Scour around pile in combined waves and current. Journal of Hydraulic Engineering. 2001; **127**(5):403-411. DOI: 10.1061/(ASCE)0733-9429(2001)127:5(403)

[45] Sumer BM, Fredsøe J. The Mechanics of Scour in the Marine Environment. Singapore: World Scientific; 2002. DOI: 10.1142/4942

[46] Rudolph D, Bos KJ, Luijendijk AP, et al. Scour around offshore structures—Analysis of field measurements. In: Proceedings of the 2nd International Conference on Scour and Erosion; Vol. 1; 2004. pp. 14-17

[47] Rudolph D, Bos K. Scour around a monopile under combined wave-current conditions and low KC-numbers. In: Proceedings of the Sixth International Conference on Scour and Erosion; 2006. pp. 582-588

[48] Qi WG, Gao FP. Equilibrium scour depth at offshore monopile foundation in combined waves and current. Science China Technological Sciences. 2014; **57**(5):1030-1039. DOI: 10.1007/s11431-014-5538-9

[49] Sumer BM, Petersen TU, Locatelli L, et al. Backfilling of a scour hole around a pile in waves and current. Journal of Waterway, Port, Coastal, and Ocean Engineering. 2013;**139**(1):9-23.

DOI: 10.1061/(ASCE)WW.1943-5460.0000161

[50] Heller V. Scale effects in physical hydraulic engineering models. Journal of Hydraulic Research. 2011;**49**(3):293-306. DOI: 10.1080/00221686.2011.578914

[51] Ettema R, Kirkil G, Muste M. Similitude of large-scale turbulence in experiments on local scour at cylinders. Journal of Hydraulic Engineering. 2006;**132**(1):33-40. DOI: 10.1061/(ASCE)0733-9429(2006)132:1(33)

[52] Ettema R, Melville BW, Barkdoll B. Scale effect in pier-scour experiments. Journal of Hydraulic Engineering. 1998;**124**(6):639-642. DOI: 10.1061/(ASCE)0733-9429(1998)124:6(639)

[53] Melville BW, Chiew YM. Time scale for local scour at bridge piers. Journal of Hydraulic Engineering. 1999;**125**(1):59-65. DOI: 10.1061/(ASCE)0733-9429(1999)125:1(59)

[54] Sheppard DM, Odeh M, Glasser T. Large scale clear-water local pier scour experiments. Journal of Hydraulic Engineering. 2004;**130**(10):957-963. DOI: 10.1061/(ASCE)0733-9429(2004)130:10(957)

[55] Lee S, Sturm T. Effect of sediment size scaling on physical modeling of bridge pier scour. Journal of Hydraulic Engineering. 2009;**135**(10):793-802. DOI: 10.1061/(ASCE)HY.1943-7900.0000091

[56] Negro V, López-Gutiérrez JS, Esteban MD, Matutano C. Uncertainties in the design of support structures and foundations for offshore wind turbines. Renewable Energy. 2014;**63**:125-132. DOI: 10.1016/j.renene.2013.08.041

[57] Qi WG, Li YX, Xu K, Gao FP. Physical modelling of local scour at twin piles under combined waves and current. Coastal Engineering. 2019;**143**:63-75. DOI: 10.1016/j.coastaleng.2018.10.009

[58] Briaud JL, Ting FCK, Cheng HC, Gudavalli R, Perugu S, Wei GS. SRICOS: Prediction of scour rate in cohesive soils at bridge piers. Journal of Geotechnical and Geoenvironmental Engineering. 1999;**125**(4):237-246. DOI: 10.1061/(ASCE)1090-0241(1999)125:4(237)

[59] Sumer BM, Christiansen N, Fredsoe J. Time scale of scour around a vertical pile. In: Proceedings of the Second International Offshore and Polar Engineering Conference; San Francisco; 1992. pp. 308-315

[60] Soulsby R. Dynamics of Marine Sands. UK: Thomas Telford; 1997

[61] Petersen TU, Sumer BM, Fredsøe J. Time scale of scour around a pile in combined waves and current. In: International Conference on Coastal Engineering; 2012. pp. 971-988

[62] Dyrseth S. Time scales for scour below pipelines and around vertical piles in nonlinear random waves and current [Master thesis]. Trondheim: Norwegian University of Science and Technology; 2015

[63] Chen B, Li S. Experimental study of local scour around a vertical cylinder under wave-only and combined wave-current conditions in a large-scale flume. Journal of Hydraulic Engineering. 2018;**144**(9):04018058. DOI: 10.1061/(ASCE)HY.1943-7900.0001502

[64] Harris J, Whitehouse RJS, Benson T. The time evolution of scour around offshore structures. ICE-Maritime Engineering. 2010;**163**(1):3-17. DOI: 10.1680/maen.2010.163.1.3

[65] Hartvig PA, Thomsen JMC, Frigaard P, et al. Experimental study of the development of scour and backfilling. Coastal Engineering Journal.

2010;**52**(02):157-194. DOI: 10.1142/S0578563410002154

[66] Sørensen SPH, Ibsen LB, Frigaard P. Experimental evaluation of backfill in scour holes around offshore monopiles. In: Frontiers in Offshore Geotechnics II. London: Taylor & Francis Group; 2010. pp. 635-640

[67] Sørensen SPH, Ibsen LB. Assessment of foundation design for offshore monopiles unprotected against scour. Ocean Engineering. 2013;**63**: 17-25. DOI: 10.1016/j.oceaneng.2013.01.016

[68] Reese LC, Cox WR Koop FD. Analysis of laterally loaded piles in sand. In: Proceedings of the Offshore Technology Conference; Houston, TX; 1974. p. 2080

[69] O'Neill MW, Murchison JM. An Evaluation of p-y Relationships in Sands, Report to American Petroleum Institute. Houston, TX, USA: University of Houston; 1983

[70] Suryasentana SK, Lehane BM. Numerical derivation of CPT-based p-y curves for piles in sand. Géotechnique. 2014;**64**(3):186-194. DOI: 10.1680/geot.13.P.026

[71] Zhu B, Sun YX, Chen RP, Guo WD, Yang YY. Experimental and analytical models of laterally loaded rigid monopiles with hardening p-y curves. Journal of Waterway, Port, Coastal, and Ocean Engineering. 2015;**141**(6): 04015007. DOI: 10.1061/(ASCE)WW.1943-5460.0000310

[72] American Petroleum Institute. Geotechnical and Foundation Design Considerations, ANSI/API Recommended Practice 2 GEO. 1st ed; 2011

[73] Qi WG, Gao FP, Randolph MF, Lehane BM. Scour effects on p-y curves for shallowly embedded piles in sand. Géotechnique. 2016;**8**:648-660. DOI: 10.1680/jgeot.15.P.157

[74] Lin C, Bennett C, Han J, Parsons RL. Scour effects on the response of laterally loaded piles considering stress history of sand. Computers and Geotechnics. 2010;**37**:1008-1014. DOI: 10.1016/j.compgeo.2010.08.009

[75] Lin C, Han J, Bennett C, Parsons RL. Analysis of laterally loaded piles in sand considering scour hole dimensions. Journal of Geotechnical and Geoenvironmental Engineering. 2014;**140**:04014024. DOI: 10.1061/(ASCE)GT.1943-5606.0001111

[76] Yang XF, Zhang CR, Huang MS, Yuan JY. Lateral loading of a pile using strain wedge model and its application under scouring. Marine Georesources & Geotechnology. 2017;**36**(3):340-350. DOI: 10.1080/1064119X.2017.1317889

[77] Tseng WC, Kuo YS, Chen JW. An investigation into the effect of scour on the loading and deformation responses of monopile foundations. Energies. 2017;**10**(8):1190. DOI: 10.3390/en10081190

[78] Sørensen SPH. Soil-structure interaction for non-slender, large-diameter offshore monopiles [PhD thesis]. Aalborg, Denmark: Aalborg University; 2012

[79] Lin C. Wu R. Evaluation of vertical effective stress and pile lateral capacities considering scour-hole dimensions. Canadian Geotechnical Journal. 2018;**56**(1):135-143. DOI: 10.1139/cgj-2017-0644

[80] Bekken L. Lateral behavior of large diameter offshore monopile foundations for wind turbines [PhD thesis]. TU Delft: Delft University of Technology; 2009

[81] Byrne BW, McAdam R, Burd HJ, et al. New design methods for large

diameter piles under lateral loading for offshore wind applications. In: Proceedings of 3rd International Symposium on Frontiers in Offshore Geotechnics. Oslo: CRC Press; 2015. pp. 1-6

[82] Gao FP, Li JH, Qi WG, Hu C. On the instability of offshore foundations: theory and mechanism. Science China - Physics Mechanics & Astronomy. 2015; **58**(12):124701. DOI: 10.1007/s11433-015-5745-9

[83] Qi WG, Gao FP. Numerical study of local scour effects on the lateral pile-soil interaction. In: Scour and Erosion: Proceedings of the 8th International Conference on Scour and Erosion; Oxford, UK; 12–15 September 2016. pp. 293-300

[84] Poulos H, Hull T. The role of analytical geomechanics in foundation engineering. In: Foundation Engineering: Current Principles and Practices. Reston, VA: ASCE 2; 1989. pp. 1578-1606

[85] Zhang CR, Zhang X, Huang MS, Tang HW. Responses of caisson-piles foundations to long-term cyclic lateral load and scouring. Soil Dynamics and Earthquake Engineering. 2019;**119**: 62-74. DOI: 10.1016/j.soildyn.2018.12.026

[86] Achmus M, Kuo YS, Abdel-Rahman K. Numerical investigation of scour effect on lateral resistance of windfarm monopiles. In: The Twentieth International Offshore and Polar Engineering Conference. Beijing, China: International Society of Offshore and Polar Engineers; 2010. pp. 619-623

[87] Bisoi S, Haldar S. Dynamic analysis of offshore wind turbine in clay considering soil-monopile-tower interaction. Soil Dynamics and Earthquake Engineering. 2014;**63**:19-35. DOI: 10.1016/j.soildyn.2014.03.006

[88] Shadlou M, Bhattacharya S. Dynamic stiffness of monopiles supporting offshore wind turbine generators. Soil Dynamics and Earthquake Engineering. 2016;**88**:15-32. DOI: 10.1016/j.soildyn.2016.04.002

[89] Kallehave D, Byrne BW, LeBlanc Thilsted C, Mikkelsen KK. Optimization of monopiles for offshore wind turbines. Philosophical Transactions of the Royal Society A - Mathematical Physical and Engineering Sciences. 2015;**373**: 20140100. DOI: 10.1098/rsta.2014.0100

[90] Prendergast LJ, Gavin K, Doherty P. An investigation into the effect of scour on the natural frequency of an offshore wind turbine. Ocean Engineering. 2015; **101**:1-11. DOI: 10.1016/j.oceaneng.2015.04.017

[91] Prendergast LJ, Reale C, Gavin K. Probabilistic examination of the change in eigen frequencies of an offshore wind turbine under progressive scour incorporating soil spatial variability. Marine Structures. 2018;**57**:87-104. DOI: 10.1016/j.marstruc.2017.09.009

[92] Damgaard M, Andersen LV, Ibsen LB. Dynamic response sensitivity of an offshore wind turbine for varying subsoil conditions. Ocean Engineering. 2015;**101**:227-234. DOI: 10.1016/j.oceaneng.2015.04.039

[93] Damgaard M, Ibsen LB, Andersen LV, Andersen JK. Cross-wind modal properties of offshore wind turbines identified by full scale testing. Journal of Wind Engineering and Industrial Aerodynamics. 2013;**116**: 94-108. DOI: 10.1016/j.jweia.2013.03.003

[94] Schafhirt S, Page A, Eiksund GR, Muskulus M. Influence of soil parameters on the fatigue lifetime of offshore wind turbines with monopile support structure. Energy Procedia. 2016;**94**:347-356. DOI: 10.1016/j.egypro.2016.09.194

[95] Rezaei R, Duffour P, Fromme P. Scour influence on the fatigue life of operational monopile-supported offshore wind turbines. Wind Energy. 2018;**21**(9):683-696. DOI: 10.1002/we.2187

[96] Lehane BM, Pedram B, Doherty JA, Powrie W. Improved performance of monopiles when combined with footings for tower foundations in sand. Journal of Geotechnical and Geoenvironmental Engineering. 2014;**140**:04014027. DOI: 10.1061/(ASCE)GT.1943-5606.0001109

[97] Anastasopoulos I, Theofilou M. Hybrid foundation for offshore wind turbines: Environmental and seismic loading. Soil Dynamics and Earthquake Engineering. 2016;**80**:192-209. DOI: 10.1016/j.soildyn.2015.10.015

[98] Stone KJL, Arshi HS, Zdravkovic L. Use of a bearing plate to enhance the lateral capacity of monopiles in sand. Journal of Geotechnical and Geoenvironmental Engineering. 2018;**144**(8):04018051. DOI: 10.1061/(ASCE)GT.1943-5606.0001913

[99] Wang X, Zeng X, Li X, Li J. Investigation on offshore wind turbine with an innovative hybrid monopile foundation: an experimental based study. Renewable Energy. 2019;**132**:129-141. DOI: 10.1016/j.renene.2018.07.127

[100] Whitehouse RJS, Sutherland J, Harris JM. Evaluating scour at marine gravity foundations. In: Proceedings of the ICE-Maritime Engineering; 2011. pp. 143-157

[101] Qi WG, Gao FP. Wave induced instantaneously-liquefied soil depth in a non-cohesive seabed. Ocean Engineering. 2018;**153**:412-423. DOI: 10.1016/j.oceaneng.2018.01.107

[102] Qi WG, Li CF, Jeng DS, Gao FP, Liang Z. Combined wave-current induced excess pore-pressure in a sandy seabed: Flume observations and comparisons with theoretical models. Coastal Engineering. 2019;**147**:89-98. DOI: 10.1016/j.coastaleng.2019.02.006

[103] Lin Z, Pokrajac D, Guo Y, Jeng DS, Tang T, Rey N, et al. Investigation of nonlinear wave-induced seabed response around mono-pile foundation. Coastal Engineering. 2017;**121**:197-211. DOI: 10.1016/j.coastaleng.2017.01.002

[104] Zhao HY, Jeng DS, Liao CC, Zhu JF. Three-dimensional modeling of wave-induced residual seabed response around a mono-pile foundation. Coastal Engineering. 2017;**128**:1-21. DOI: 10.1016/j.coastaleng.2017.07.002

[105] Zhu B, Ren J, Ye GL. Wave-induced liquefaction of the seabed around a single pile considering pile-soil interaction. Marine Georesources & Geotechnology. 2018;**36**(1):150-162. DOI: 10.1080/1064119X.2017.1340374

[106] Duan LL, Jeng DS, Wang D. PORO-FSSI-FOAM: Seabed response around a mono-pile under natural loadings. Ocean Engineering. 2019;**184**:239-254. DOI: 10.1016/j.oceaneng.2019.05.024

[107] Sui TT, Zhang C, Guo YK, Zheng JH, Jeng DS, Zhang JS, et al. Three-dimensional numerical model for wave-induced seabed response around mono-pile. Ships and Offshore Structures. 2016;**11**(6):667-678. DOI: 10.1080/17445302.2015.1051312

[108] Li Y, Ong MC, Tang T. Numerical analysis of wave-induced poro-elastic seabed response around a hexagonal gravity-based offshore foundation. Coastal Engineering. 2018;**136**:81-95. DOI: 10.1016/j.coastaleng.2018.02.005